Mituyoshi et al. reported that continuous intravenous PGE1 administration resolved the spasm and narrowing of the superior mesenteric artery in NOMI patients. In our study, ten patients received continuous intravenous PGE1 administration. A larger study is required to understand the efficacy of continuous intravenous PGE1 administration for additional postoperative treatment of NOMI.

Our study is the largest study to date to evaluate the clinical features and prognostic factors of NOMI. Based on our findings, we conclude that the POSSUM score can be used to predict the outcome of NOMI patients who undergo surgery. Surgery followed by additional postoperative treatment may improve the prognosis of NOMI. It is difficult and impractical to use randomized controlled trials to determine the usefulness of surgery for NOMI, and retrospective studies from multiple institutions may be required to provide sufficient data. Our findings offer useful information for determining the treatment strategy for NOMI.

Acknowledgments We wish to thank the following institutions for participating in the investigation: Iizuka Hospital, Imari Arita Kyoritsu Hospital, Eikou Hospital, Oita Medical Center, Oita Prefecture Hospital, Oita Red Cross Hospital, Onga Hospital, Kitakyushu Municipal Medical Center, Kakizoe Hospital, National Kyushu Cancer Center, Saiseikai Karatsu Hospital, Saiseikai Fukuoka General Hospital, Saiseikai Yahata General Hospital, Shinnakama Hospital, Nakatsu Municipal Hospital, Hita Central Hospital, Hiroshima Red Cross Hospital & Atomic Bomb Survivors Hospital, Fukuoka City Hospital, National Fukuoka-Higashi Medical Center, Steel Memorial Yawata Hospital, Beppu Medical Center, Matsuyama Red Cross Hospital, and Munakata Medical Association Hospital.

References

1. Ende N. Infarction of the bowel in cardiac failure. N Engl J Med. 1958;258:879–881.
2. John AS, Tuerff SD, Kerstein MD. Nonocclusive mesenteric infarction in hemodialysis patients. J Am Coll Surg 2000; 190:84–88.
3. Mitsuyoshi A, Obama K, Shinkura N, Ito T, Zaima M. Survival in nonocclusive mesenteric ischemia: Early diagnosis by multidetector row computed tomography and early treatment with continuous intravenous high-dose prostaglandin E1. Ann Surg 2007;246:229–235
4. Quiroga B, Verde E, Abad S, Vega A, Goicoechea M, Reque J, López-Gómez JM, Luño J. Detection of patients at high risk for non-occlusive mesenteric ischemia in hemodialysis. J Surg Res. 2013;180:51–55.
5. AGA technical review on intestinal ischemia. Gastroenterology 2000;118:954–968.
6. American Gastroenterological Association medical position statement: guidelines on intestinal ischemia. Gastroenterology 2000;118:951–953.
7. Brandt LJ, Boley SJ. Nonocclusive Mesenteric Ischemia. Annu Rev Med 1991;42:107–117
8. Boley SJ, Sprayrgen S, Sieglman SS, Vieth FJ. Initial results from an aggressive roentgenological approach to acute mesenteric ischemia. Surgery 1977;82:848–855
9. Ward D, Vernava AM, Kaminski DL, Ure T, Peterson G, Garvin P, Arends TW, Longo WE. Improved Outcome by Identification of High-Risk Nonocclusive Mesenteric Ischemia, Aggressive Reexploration, and Delayed Anastomosis. Am J Surg 1995;170: 577–581.
10. Heer FW, Silen W, French SW. Intestinal gangrene without apparent vascular occlusion. Am J Surg. 1965;110:231–238.
11. Fogarty JT, Fletcher SW. Genesis to nonocclusive mesenteric ischemia. Am J Surg. 1966;111:130–137.
12. Copeland GP, Jones D, Walters M. POSSUM: a scoring system for surgical audit. British Journal of Surgery 1991;78(3):355–60.
13. Hirasawa H, Oda S, Nakamura M, Watanabe E, Shiga H, Matsuda K. Continuous hemodiafiltration with a cytokine-adsorbing hemofilter for sepsis. Blood Purif. 2012;34(2):164–70.
14. Sato H, Oshima K, Arakawa K, Kobayashi K, Yamazaki H, Suto Y, Takeyoshi I. Direct hemoperfusion with a polymyxin B-immobilized cartridge in intestinal warm ischemia reperfusion. World J Gastroenterol. 2008 ;14(35):5436–41.
15. Howard TJ, Plaskon LA, Wiebke EA, Wilcox MG, Madura JA. Nonocclusive mesenteric ischemia remains a diagnostic dilemma. Am J Surg. 1996;171:405–408.
16. Trompeter M, Brazda T, Remy CT, Vestring T, Reimer P. Nonocclusive mesenteric ischemia: etiology, diagnosis, and interventional therapy. Eur Radiol. 2002;12(5):1179–1187.
17. Lock G, Scholmerich J. Nonocclusive mesenteric ischemia. Hepatogastroenterology. 1995;42:234–239.
18. Bender JS, Ranter LE, Magnuson TH, Zenilman ME. Acute abdomen in the hemodialysis patient population. Surgery 1995;117:494–497.
19. Wittenberg J, Athanasoulis CA, Williams LF, Paredes S, O'sullvian P, Brown B. Ischemic colitis. Radiology and pathophysiology. Am J Roentgenol Radium Ther Nucl Med. 1975;123(2):287–300.
20. Clinical features and management of hepatic portal venous gas: four case reports and cumulative review of the literature. Arch Surg 2001;136 (12) 1410–1414.
21. Liebman PR, Patten MT, Manny J, Benfield JR, Hechtman HB. Hepatic-portal venous gas in adults: Etiology, pathophysiology and clinical significance. Ann Surg 1978;187: 281–287.
22. Sotiriadis J, Brandt LJ, Behin DS, Southern WN. Ischemic Colitis Has a Worse Prognosis When Isolated to the Right Side of the Colon. Am J Gastroenterol 2007;102(10):2247–2252.
23. Aliosmanoglu I, Gil M, Kapan M, Arikanoglu Z, Taskesen F, Basol O, Aldemir M. Risk factors effecting mortality in acute mesenteric ischemia and mortality rates: a single center experience. Int Surg 2013;98:76–81.
24. Knaus WA, Draper EA, Wagner DP, Zimmerman JE. APACHE II: A severity of disease classification system. Critical Care Medicine 1985;13:818–829.
25. Hsu HP, Shan YS, Hsieh YH, Sy ED, Lin PW. Impact of Etiologic Factors and APACHE II and POSSUM Scores in Management and Clinical Outcome of Acute Intestinal Ischemic Disorders after Surgical Treatment. World J Surg 2006;30: 2152–2162
26. Mohil RS, Bhatnagar D, Bahadur L Rajneesh, Dev DK, Magan M. POSSUM and P-POSSUM for risk-adjusted audit of patients undergoing emergency laparotomy. Br J Surg 2004;91 500–503.
27. Jones DR, Copelans GP, de Cossart L. Comparison of POSSUM with APACHE II for prediction of outcome from a surgical high dependency unit. Br J Surg 1992;79:1293–1296.

Ann Surg Oncol (2014) 21:3063–3068
DOI 10.1245/s10434-014-3686-6

Annals of
SURGICAL ONCOLOGY
OFFICIAL JOURNAL OF THE SOCIETY OF SURGICAL ONCOLOGY

ORIGINAL ARTICLE – HEPATOBILIARY TUMORS

Effect of Body Composition on Outcomes after Hepatic Resection for Hepatocellular Carcinoma

Shinji Itoh, MD, PhD[1], Ken Shirabe, MD, PhD, FACS[1], Yoshihiro Matsumoto, MD[1], Shohei Yoshiya, MD[1], Jun Muto, MD[1], Norifumi Harimoto, MD, PhD[1], Yo-ichi Yamashita, MD, PhD[1], Toru Ikegami, MD, PhD, FACS[1], Tomoharu Yoshizumi, MD, FACS[1], Akihiro Nishie, MD, PhD[2], and Yoshihiko Maehara, MD, PhD, FACS[1]

[1]Department of Surgery and Science, Graduate School of Medical Sciences, Kyushu University, Fukuoka, Japan; [2]Department of Clinical Radiology, Graduate School of Medical Sciences, Kyushu University, Fukuoka, Japan

ABSTRACT

Purpose. To evaluate the effect of body composition on outcomes after hepatic resection for patients with hepatocellular carcinoma (HCC).

Methods. We performed 190 hepatic resections for HCC and divided the patients into 2 groups on the basis of visceral fat area (VFA), assessed by computed tomographic measurement at the level of the umbilicus, into high VFA (H-VFA) ($n = 106$) and low VFA (L-VFA) ($n = 84$) groups. We compared the surgical outcomes between the two groups.

Results. L-VFA was significantly correlated with a lower body mass index, sarcopenia, lower serum albumin, and liver cirrhosis. There was no difference in the incidence of postoperative complications and mortality between the 2 groups. Patients in the L-VFA group had a significantly poorer prognosis than those in the H-VFA group in terms of both overall ($P = 0.043$) and recurrence-free ($P = 0.001$) survival. The results of multivariate analysis showed that sarcopenia rather than L-VFA was an independent and prognostic indicator after hepatic resection with HCC.

Conclusions. Body composition is an important factor affecting cancer outcomes after hepatic resection for HCC in Japan.

Hepatocellular carcinoma (HCC) is the most frequent epithelial cancer of the liver, one of the most common cancers worldwide, and a major cause of death in many countries, especially Japan.[1,2] Hepatic resection remains one of the most common effective treatments for HCC.[3–5] However, a considerable number of patients develop intrahepatic recurrence, and although surgical techniques have recently been improved, postoperative morbidity in patients with HCC remains high.[5–10]

Body mass index (BMI) has been widely used as an indicator of obesity and is easily calculated using a patient's height and weight. The effects of BMI on surgical outcome are controversial in patients who undergo abdominal surgery.[11–13] Evidence has emerged that BMI is not the most sensitive predictor of outcomes after abdominal surgery and that measures of visceral fat area (VFA) better identify high-risk patients.[14,15] However, this issue is also contentious. Recently, several body composition features have been associated with cancer outcomes, and we previously reported that sarcopenia, or severe muscle depletion, was a marker of poor prognosis after hepatic resection in patients with HCC.[16]

To our knowledge, no previous data have been published on VFA for patients undergoing hepatic resection for HCC. Therefore, we retrospectively investigated the relationship between VFA and surgical outcomes after hepatic resection in patients with HCC.

MATERIALS AND METHODS

Patients

We included 190 patients who underwent hepatic resection for initial HCC without simultaneous procedures such as biliary reconstruction, gastrointestinal resection, or colorectal resection, at the Department of Surgery and Science, Kyushu University Hospital, between 2004 and

First Received: 16 January 2014;
Published Online: 10 April 2014

S. Itoh, MD, PhD
e-mail: itoshin@surg2.med.kyushu-u.ac.jp

2009. Patients' clinical, surgical, and pathological data were collected retrospectively from the institute's database, as well as from each patient's medical chart. All patients underwent preoperative computed tomography (CT). The degree of proportional visceral adiposity and skeletal muscle mass was measured from the patients' preoperative CT images. VFA was measured from a single axial slice at the level of the umbilicus.[17,18] VFA was calculated by measuring pixels with densities of −190 to −30 HU (Hounsfield units). A transverse CT image at the third lumbar vertebra (L3) in the inferior direction was assessed from each scan, and skeletal muscle was identified and quantified by HU thresholds of −29 to +150 (water is defined as 0 HU and air as 1000 HU).[16] Multiple muscles were quantified, including the psoas, erector spinae, quadratus lumborum, transversus abdominis, external and internal oblique abdominal muscles, and rectus abdominis muscle. CT measurements were calibrated with water and air at fixed intervals, and VFA and skeletal muscle mass were measured by manual outlining on the CT images and checked by the radiologist.

The details of the surgical techniques and patient selection criteria have been previously reported.[10] Selection criteria for hepatic resection were as follows: ascites not detected or controllable by diuretics; serum total bilirubin level <2.0 mg/ml; and indocyanine green dye retention test at 15 min of <40 %. Parenchymal transection was performed by the Cavitron Ultrasonic Surgical Aspirator (CUSA system; Valleylab, Boulder, CO, USA) and a monopolar dissecting sealer (TissueLink; TissueLink Medical, Dover, NH, USA). Inflow vascular control was performed with intermittent hemi- or total Glisson sheath occlusion.[19]

Postoperative morbidity was graded according to the Dindo-Clavien classification, and we analyzed postoperative complications of Clavien grade IIIa or higher.[20] Patients were strictly followed after the hepatic resection, with monthly measurement of the levels of α-fetoprotein and des-gamma carboxy prothrombin, as well as monthly ultrasonography. Dynamic CT was performed every 6 months by radiologists, and an angiographic examination was performed after admission when there was a strong suspicion of disease recurrence.

Statistical Analysis

Continuous variables without normal distribution were compared by the Mann–Whitney *U*-test. Categorical variables were compared by the χ^2 test or Fisher's exact test. The Cox proportional hazard model was used for univariate analysis of survival data including covariates that were significant at $P < 0.05$ in the model. The overall survival and disease-free survival rates were calculated by the Kaplan–Meier (product limit) estimator and compared by the log rank test. Differences were considered significant at $P < 0.05$. All statistical analyses were performed by StatView 5.0 (Abacus Concepts, Berkeley, CA, USA).

RESULTS

The BMI groupings were as follows: BMI <18.5 kg/m^2 (underweight), 15 patients; BMI ≥18.5 kg/m^2 to <25 kg/m^2 (normal weight), 130 patients; BMI 25 to <30 kg/m^2 (overweight), 41 patients; and BMI ≥30 kg/m^2 (obese), 4 patients, categorized according to World Health Organization criteria.[21] We observed a significant positive correlation between BMI and VFA ($P < 0.0001$; $R^2 = 0.562$), although a wide range of VFA results existed within each BMI class (Fig. 1).

The median VFA of all patients was 98.4 cm^2 (range 17.9–410.5 cm^2) and in male patients was 108.0 cm^2 (range 17.9–410.5 cm^2), which was more than that in female patients (median 76.0; range 32.2–220.5 cm^2; $P = 0.010$). Cutoff values for VFA associated with overall survival were defined as 103 cm^2 for men and 69 cm^2 for women, which is recognized as a measure of metabolic abnormalities in

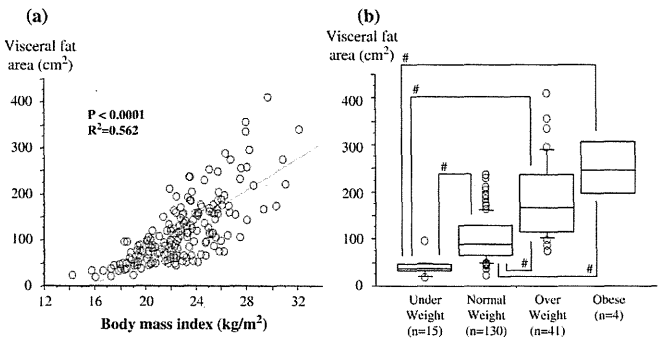

FIG. 1 VFA distribution according to body mass index as a continuous variable (**a**) or as a categorical variable (**b**). $^{\#}P < 0.01$

TABLE 1 Characteristics of patients with HCC who underwent hepatic resection

Characteristic	Low VFA ($n = 84$)	High VFA ($n = 106$)	P
Age, year	68 (34–87)	69 (31–83)	0.918
Sex, M/F	67/17	79/27	0.395
BMI, kg/m^2	20.5 (14.2–26.1)	24.0 (18.7–32.1)	<0.001
Sarcopenia	52 (61.9 %)	25 (23.5 %)	<0.001
Diabetes mellitus	25 (39.7 %)	36 (34.6 %)	0.538
Albumin, g/dl	3.9 (2.1–4.6)	4.1 (2.8–5.0)	0.007
Total bilirubin, mg/dl	0.7 (0.4–2.0)	0.7 (0.1–2.6)	0.527
Platelets, $\times 10^4$/mm^3	14.3 (5.2–41.3)	15.6 (4.1–36.3)	0.141
$ICGR_{15}$, %	13.4 (3.3–39.0)	13.4 (1.6–34.6)	0.883
Total cholesterol, mg/dl	169 (105–254)	165 (107–305)	0.326
Liver cirrhosis	33 (39.2 %)	27 (25.4 %)	0.041
Tumor size, cm	3.2 (1.0–15.0)	3.3 (1.0–16.5)	0.794
Solitary/multiple	44/40	70/36	0.073
Poorly differentiation	28 (33.3 %)	28 (26.4 %)	0.298
Microvascular invasion	29 (34.5 %)	36 (33.9 %)	0.935
AFP, ng/ml	16.2 (0.8–170668)	9.1 (0–577660)	0.171
DCP, mAU/ml	44.0 (2.4–75000)	77.0 (2.0–75000)	0.194
Anatomical resection	55 (65.4 %)	66 (62.2 %)	0.674
Operation time, min	325 (117–613)	370 (147–770)	0.142
Blood loss, g	454 (1–4800)	500 (15–3152)	0.280
Blood transfusion	8 (9.5 %)	13 (12.2 %)	0.549
Any complication	17 (20.2 %)	19 (17.9 %)	0.686
Wound infection	11 (13.0 %)	9 (8.4 %)	0.304
Intra-abdominal infection	5 (5.9 %)	3 (2.8 %)	0.469
Bile leakage	3 (3.5 %)	5 (4.7 %)	>0.999
Ascites	3 (3.5 %)	1 (0.9 %)	0.323
30 days mortality	0 (0 %)	0 (0 %)	>0.999
90 days mortality	0 (0 %)	0 (0 %)	>0.999

VFA visceral fat area, *BMI* body mass index, *$ICGR_{15}$* indocyanine green dye retention test at 15 min, *AFP* α-fetoprotein, *DCP* des-gamma carboxy prothrombin

Japan.[22] We divided the study population into two groups according to high VFA (H-VFA) or low VFA (L-VFA). Cutoff values for skeletal muscle were defined as 43.75 cm^2/m^2 for men and 41.10 cm^2/m^2 for women.[16] On the basis of this cutoff, patients were assigned to one of two groups, depending on the presence or absence of sarcopenia.

The clinicopathological characteristics for patients in the L-VFA group ($n = 84$) and the H-VFA group ($n = 106$) are shown in Table 1. Serum albumin levels in the L-VFA group were significantly lower than in the H-VFA group ($P = 0.007$). The percentages of patients with liver cirrhosis ($P = 0.041$) and sarcopenia ($P < 0.001$) in the L-VFA group were significantly higher than in the H-VFA group, and no differences were noted between the two groups in terms of other liver function data, tumor factors, and surgical factors. There was no difference in the incidence of postoperative complications and mortality between the two groups.

Figure 2 shows the overall and recurrence-free survival curves after hepatic resection between the two groups. The 3-, 5-, and 7-year overall survival rates were 86.5, 78.2, and 74.3 % in the H-VFA group and 79.0, 65.3, and 45.2 % in the L-VFA group, respectively. The 3-, 5-, and 7-year recurrence-free survival rates were 54.7, 46.4, and 36.5 % in the H-VFA group and 37.3, 23.7, and 14.4 % in the L-VFA group, respectively. Patients with L-VFA had a significantly worse prognosis than those with H-VFA with respect to both overall ($P = 0.043$) and recurrence-free ($P = 0.001$) survival.

Table 2 shows the results of the univariate analysis used to identify the significant factors closely related to the long-term survival rate after hepatic resection in patients with HCC. Poor prognostic factors included L-VFA, sarcopenia, multiple tumors, microvascular invasion, and intraoperative blood transfusion. The Cox proportional hazard model was used to assess the effect of different variables on overall survival. Poor prognostic factors identified by multivariate analysis included sarcopenia, multiple tumors, microvascular invasion, and intraoperative blood transfusion; these were factors that influenced the overall survival rate in patients with HCC.

Significant prognostic factors for recurrence-free survival were L-VFA, BMI <25 kg/m^2, sarcopenia, liver cirrhosis, multiple tumors, poor differentiation, and microvascular invasion (Table 3). Multivariate analysis identified two prognostic factors (multiple tumors and microvascular invasion) that influenced recurrence-free survival.

DISCUSSION

We found that L-VFA was highly correlated with lower BMI, sarcopenia, lower serum albumin level, and liver cirrhosis. Short-term outcomes including mortality and postoperative complications were not correlated with VFA. Indicators of host factors such as sarcopenia and neutrophil-to-lymphocyte ratio, tumor factors such as tumor size, des-gamma carboxy prothrombin, expression of focal adhesion kinase, and expression of diacylglycerol kinase have previously been reported to be predictors of poor prognosis in patients with HCC.[16,23–26] Our results showed that L-VFA was not an independent predictor of poor survival after hepatic resection in patients with HCC. To our knowledge, this is the first clinical study to assess the relationships between VFA and surgical outcomes after hepatic resection in patients with HCC.

In this study, VFA was not related to tumor factors but was significantly correlated with host factors including BMI, skeletal muscle mass (sarcopenia), serum level of

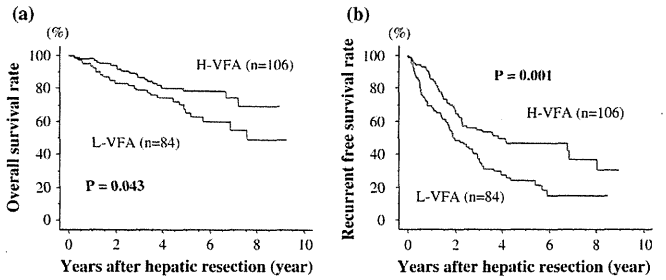

FIG. 2 **a** Overall and **b** recurrence-free survival curves after hepatic resection in patients with HCC comparing high visceral fat area (H-VFA) and low visceral fat area (L-VFA). **a** $P = 0.043$, **b** $P = 0.001$ (log rank test)

TABLE 2 Univariate and multivariate Cox proportional hazard analysis of factors related to overall survival in patients with HCC who underwent hepatic resection

Variable	Univariate			Multivariate		
	Hazard ratio	95 % CI	*P*	Hazard ratio	95 % CI	*P*
Age ≥65 year	1.58	0.84–3.03	0.158			
Male	0.99	0.50–1.95	0.993			
L-VFA	1.78	1.00–3.15	0.046	1.51	0.80–2.83	0.194
BMI <25 kg/m^2	1.93	0.86–4.31	0.106			
Sarcopenia	2.08	1.18–3.69	0.012	1.96	1.06–3.74	0.031
Albumin <3.6 g/dl	1.06	0.47–2.37	0.884			
Platelet <10.0 × 10^4/mm^3	1.75	0.90–3.44	0.097			
Liver cirrhosis	1.21	0.67–2.17	0.523			
Tumor size ≥5.0 cm	1.62	0.90–2.91	0.105			
Multiple tumors	2.17	1.23–3.84	0.007	2.34	1.31–4.18	0.003
Poorly differentiation	1.72	0.97–3.05	0.064			
Microvascular invasion	2.18	1.23–3.87	0.007	2.50	1.38–4.52	0.002
Blood loss >1,000 g	1.27	0.62–2.56	0.503			
Intraoperative blood transfusion	2.35	1.17–4.73	0.016	2.80	1.35–5.78	0.005
Postoperative complication	1.36	0.69–2.66	0.370			

CI confidence interval, *L-VFA* low visceral fat area, *BMI* body mass index

albumin, and liver cirrhosis. Likewise, we previously reported that BMI and skeletal muscle mass were not related to tumor factors.[13,16] Taken together, this suggests that body composition would not correlate with tumor factors but would be related to host factors.

Several recent reports have suggested that VFA is more strongly associated with postoperative intra-abdominal infectious complications in patients with gastric cancer and colon cancer.[14,15] However, Gaujoux et al.[27] found that BMI and VFA were not correlated with postoperative complications after pancreaticoduodenectomy for pancreatic adenocarcinoma. We previously reported that overweight status was not a risk factor for postoperative complications or mortality in patients with HCC after hepatic resection, and Saunders et al. reported that there were no differences across BMI groups in overall and specific morbidity after liver resection.[13,28] We found that VFA was significantly correlated with BMI but was not correlated with diabetes mellitus or serum total cholesterol level, which are known metabolic disorders.[29] These data indicate that there is no effect of VFA on short-term surgical outcomes after hepatic resection in patients with HCC.

Few investigators have studied the effect of VFA on long-term outcomes after surgery. Gaujoux et al.[27] found that BMI and VFA were not correlated with prognosis after pancreaticoduodenectomy in terms of both overall and recurrence-free survival for 328 patients with pancreatic adenocarcinoma. Van Vledder et al.[30] reported that VFA did not predict overall survival after hepatic resection in patients with colorectal liver metastases. In our study, we found that L-VFA was a significantly worse long-term prognostic factor for survival in patients with HCC after hepatic resection in univariate analysis. However, the results of the multivariate analysis showed sarcopenia

TABLE 3 Univariate and multivariate Cox proportional hazard analysis of factors related to recurrence-free survival in patients with HCC who underwent hepatic resection

Variable	Univariate			Multivariate		
	Hazard ratio	95 % CI	*P*	Hazard ratio	95 % CI	*P*
Age ≥65 year	1.16	0.75–1.79	0.483			
Male sex	1.17	0.73–1.86	0.511			
L-VFA	1.85	1.27–2.68	0.001	1.44	0.94–2.21	0.086
BMI <25 kg/m^2	2.08	1.25–3.45	0.004	1.19	0.66–2.13	0.557
Sarcopenia	1.62	1.11–2.36	0.012	1.30	0.85–2.00	0.215
Albumin <3.6 g/dl	1.01	0.61–1.69	0.941			
Platelet <10.0 × 10^4/mm^3	1.30	0.79–2.13	0.300			
Liver cirrhosis	1.52	1.03–2.24	0.031	1.27	0.85–1.90	0.240
Tumor size ≥5.0 cm	1.47	0.99–2.19	0.053			
Multiple tumors	2.57	1.76–3.75	<0.001	2.40	1.63–3.53	<0.001
Poor differentiation	1.48	1.00–2.20	0.046	1.19	0.79–1.79	0.392
Microvascular invasion	1.54	1.05–2.27	0.026	1.69	1.12–2.56	0.019
Blood loss >1,000 g	1.02	0.61–1.70	0.918			
Intraoperative blood transfusion	1.35	0.75–2.42	0.303			
Postoperative complication	1.08	0.67–1.75	0.725			

CI confidence interval, *L-VFA* low visceral fat area, *BMI* body mass index

rather than L-VFA to be an independent and prognostic indicator after hepatic resection with HCC. Patients with relatively H-VFA may have more sufficient nutritional and physiologic reserves than L-BMI patients.

An abundance of experimental and epidemiologic evidence has demonstrated that metabolic regulation and the immune response are highly integrated and that the proper functioning of each is dependent on the other.[31] Serum albumin level is a marker for nutritional status, and we found that the serum albumin level in the H-VFA group was significantly higher than that in the L-VFA group.[32] However, the percentage of patients with liver cirrhosis in the L-VFA group was significantly higher than in the H-VFA group. The relationship between the serum level of albumin and VFA is complicated in the presence of underlying liver disease. Recent studies have measured body fat distribution including abdominal wall fat, hip girdle fat, visceral fat, and abdominal depth measuring intra-abdominal fat using a simple radiologic analysis and found that increased body fat was advantageous for long-term survival after pancreaticoduodenectomy in 408 patients with pancreatic adenocarcinoma.[33] Additional studies are required to clarify the relationship between VFA and nutritional status in patients with liver disease.

It was interesting that sarcopenia was a stronger prognostic factor than L-VFA for overall survival after hepatic resection of HCC. Sarcopenia is defined as a low level of skeletal muscle mass—a level below the healthy young adult mean.[34] Although sarcopenia is associated with aging, it can also be present as a result of chronic diseases and malignancy.[30,35] We previously found that sarcopenia was significantly correlated with lower albumin levels and BMI, and that it was an independent predictor of poor survival after hepatic resection in patients with HCC.[16] In our data including VFA and sarcopenia, L-VFA and sarcopenia were not independent predictors for recurrence-free survival, but sarcopenia rather than L-VFA was an independent predictor for overall survival after hepatic resection in patients with HCC. This cutoff value of VFA is recognized as a measure of metabolic abnormalities in Japan.[22] Patients with H-VFA might be assumed to have good nutritional status, but all patients with L-VFA might not have poor nutritional status. This multivariate data may suggest that skeletal muscle is a better parameter than visceral fat to describe malnutrition.

Our study has several limitations. It is a single institutional and retrospective review; we included a relatively small number of patients, especially those with BMI ≥30 kg/m^2 and BMI <18.5 kg/m^2; and the cutoff value in this study is an indication for Japanese patients, and the cutoff value of VFA might differ in patients with liver disease. These limitations will need to be addressed in multi-institutional reviews and possible clinical studies.

In conclusion, our study found that VFA did not have an effect on short-term outcomes including postoperative mortality and complications after hepatic resection in patients with HCC. Better nutritional status, including H-VFA, might be advantageous for long-term survival after hepatic resection for HCC in Japan.

REFERENCES

1. Bruix J, Lovet JM. Prognostic prediction and treatment strategy in hepatocellular carcinoma. *Hepatology*. 2002:35:519–24.
2. Bosch FX, Ribes J, Díaz M, et al. Primary liver cancer: worldwide incidence and trends (review). *Gastroenterology*. 2004;127: S5–16.
3. Takenaka K, Kawahara N, Yamamoto K, et al. Results of 280 liver resections for hepatocellular carcinoma. *Arch Surg*. 1996;131:71–6.
4. Shirabe K, Takeishi K, Taketomi A, et al. Improvement of long-term outcomes in hepatitis C virus antibody-positive patients with hepatocellular carcinoma after hepatectomy in the modern era. *World J Surg*. 2011:35:1072–84.
5. Itoh S, Morita K, Ueda S, et al. Long-term results of hepatic resection combined with intraoperative local ablation therapy for patients with multinodular hepatocellular carcinomas. *Ann Surg Oncol*. 2009;16:3299–307.
6. Yamashita Y-i, Taketomi A, Itoh S, et al. Longterm favorable results of limited hepatic resections for patients with hepatocellular carcinoma. *J Am Coll Surg*. 2007;205:19–26.
7. Itoh S, Fukuzawa K, Shitomi Y, et al. Impact of the VIO system in hepatic resection for patients with hepatocellular carcinoma. *Surg Today*. 2012;42:1176–82.
8. Uchiyama H, Itoh S, Higashi T, et al. A two-step hanging maneuver for a complete resection of Couinaud's segment I. *Dig Surg*. 2012;29:202–5.
9. Taketomi A, Kitagawa D, Itoh S, et al. Trends in morbidity and mortality after hepatic resection for hepatocellular carcinoma: an institute's experience with 625 patients. *J Am Coll Surg*. 2007; 204:580–7.
10. Itoh S, Shirabe K, Taketomi A, et al. Zero mortality in more than 300 hepatic resections: validity of preoperative volumetric analysis. *Surg Today*. 2012;42:435–40.
11. Merkow RP, Bilimoria KY, McCarter MD, et al. Effect of body mass index on short-term outcomes after colectomy for cancer. *J Am Coll Surg*. 2009;208:53–61.
12. Mullen JT, Davenport DL, Hutter MM, et al. Impact of body mass index on perioperative outcomes in patients undergoing major intra-abdominal cancer surgery. *Ann Surg Oncol*. 2007;15: 2164–72.
13. Itoh S, Ikeda Y, Kawanaka H, et al. The effect of overweight status on the short-term and 20-y outcomes after hepatic resection in patients with hepatocellular carcinoma. *J Surg Res*. 2012;178:640–5.
14. Sugisawa N, Tokunaga M, Tanizawa Y, et al. Intra-abdominal infectious complications following gastrectomy in patients with excessive visceral fat. *Gastric Cancer*. 2012;15:206–12.
15. Cecchini S, Cavazzini E, Marchesi F, et al. Computed tomography volumetric fat parameters versus body mass index for predicting short-term outcomes of colon surgery. *World J Surg*. 2011;35:415–23.
16. Harimoto N, Shirabe K, Yamashita YI, et al. Sarcopenia as a predictor of prognosis in patients following hepatectomy for hepatocellular carcinoma. *Br J Surg*. 2013;100:1523–30.
17. Kvist H, Chowdhury B, Sjöström L, et al. Adipose tissue volume determination in males by computed tomography and 40 K. *Int J Obes*. 1988;12:249–66.
18. Yoshizumi T, Nakamura T, Yamane M, et al. Abdominal fat: standardized technique for measurement at CT. *Radiology*. 1999; 211:283–6.
19. Pringle JH. Notes on the arrest of hepatic hemorrhage due to trauma. *Ann Surg*. 1908;48:58–62.
20. Clavien PA, Barkun J, de Oliveira ML, et al. The Clavien-Dindo classification of surgical complication: five-year experience. *Ann Surg*. 2009;250:187–96.
21. World Health Organization. Obesity: preventing and managing the global epidemic. Geneva, Switzerland: World Health Organization; 2000.
22. Kashihara H, Lee JS, Kawakubo K, et al. Criteria of waist circumference according to computed tomography-measured visceral fat area and the clustering of cardiovascular risk factors. *Circ J*. 2009;73:1881–6.
23. Mano Y, Shirabe K, Yamashita Y, et al. Preoperative neutrophil-to-lymphocyte ratio is a predictor of survival after hepatectomy for hepatocellular carcinoma: a retrospective analysis. *Ann Surg*. 2013;258:301–5.
24. Shirabe K, Itoh S, Yoshizumi T, et al. The predictors of microvascular invasion in candidates for liver transplantation with hepatocellular carcinoma—with special reference to the serum levels of des-gamma-carboxy prothrombin. *J Surg Oncol*. 2007; 95:235–40.
25. Itoh S, Maeda T, Shimada M, et al. Role of expression of focal adhesion kinase in progression of hepatocellular carcinoma. *Clin Cancer Res*. 2004;10:2812–7.
26. Takeishi K, Taketomi A, Shirabe K, et al. Diacylglycerol kinase alpha enhances hepatocellular carcinoma progression by activation of Ras-Raf-MEK-ERK pathway. *J Hepatol*. 2012;57:77–83.
27. Gaujoux S, Torres J, Olson S, et al. Impact of obesity and body fat distribution on survival after pancreaticoduodenectomy for pancreatic adenocarcinoma. *Ann Surg Oncol*. 2012;19:2908–16.
28. Saunders JK, Rosman AS, Neihaus D, et al. Safety of hepatic resections in obese veterans. *Arch Surg*. 2012;147:331–7.
29. Dindo D, Muller MK, Weber M, et al. Obesity in generalelective surgery. *Lancet*. 2003;361:2032–5.
30. van Vledder MG, Levolger S, Ayez N, et al. Body composition and outcome in patients undergoing resection of colorectal liver metastases. *Br J Surg*. 2012;99:550–7.
31. Hotamisligil GS. Inflammation and metabolic disorders. *Nature*. 2006;444:860–7.
32. Sacks GS, Dearman K, Replogle WH, et al. Use of subjective global assessment to identify nutrition-associated complications and death in geriatric long-term care facility residents. *J Am Coll Nutr*. 2000;19:570–577.
33. Pausch T, Hartwig W, Hinz U, et al. Cachexia but not obesity worsens the postoperative outcome after pancreatoduodenectomy in pancreatic cancer. *Surgery*. 2012;152(3 Suppl 1):S81–8.
34. Rolland Y, Czerwinski S, Abellan Van Kan G, et al. Sarcopenia: its assessment, etiology, pathogenesis, consequences and future perspectives. *J Nutr Health Aging*. 2008;12:433–450.
35. Lang T, Streeper T, Cawthon P, et al. Sarcopenia: etiology, clinical consequences, intervention, and assessment. *Osteoporos Int*. 2010;21:543–59.

J Gastroenterol
DOI 10.1007/s00535-014-0992-5

The Japanese Society of Gastroenterology

ORIGINAL ARTICLE—LIVER, PANCREAS, AND BILIARY TRACT

Blockade of the apelin–APJ system promotes mouse liver regeneration by activating Kupffer cells after partial hepatectomy

Shohei Yoshiya · Ken Shirabe · Daisuke Imai · Takeo Toshima · Yo-ichi Yamashita · Toru Ikegami · Shinji Okano · Tomoharu Yoshizumi · Hirofumi Kawanaka · Yoshihiko Maehara

Received: 28 March 2014 / Accepted: 4 August 2014

Abstract
Background Liver regeneration after massive hepatectomy or living donor liver transplantation is critical. The apelin–APJ system is involved in the regulation of cardiovascular function, inflammation, fluid homeostasis, the adipo-insular axis, and angiogenesis, but its function in liver regeneration remains unclear.
Methods We investigated the impact of pharmacologic blockade of the apelin–APJ system, using the specific APJ antagonist F13A on liver regeneration after hepatectomy in mice.
Results F13A-treated mice had significantly higher serum concentrations of tumor necrosis factor (TNF)-α and interleukin (IL)-6 than control mice, due to F13A-promoted activation of Kupffer cells. Compared with untreated mice, F13A enhanced the signal transducer and activator of transcription 3 and mitogen-activated protein kinase pathways, stimulated cell-cycle progression, and promoted hepatocyte proliferation and liver regeneration without inducing apoptosis or inflammation in regenerating livers. In vitro, Kupffer cells expressed APJ and were activated directly by F13A treatment, releasing TNF-α and IL-6. Moreover, F13A-treated mice had a higher survival rate than untreated mice in the extended hepatectomy model.
Conclusions F13A treatment promotes early phase liver regeneration after hepatectomy by promoting the activation of Kupffer cells and increasing serum levels of TNF-α and IL-6. F13A treatment may become a therapeutic option to facilitate efficient liver regeneration after liver surgery.

Keywords F13A · Apelin–APJ signaling · Hepatocyte proliferation · TNF-α · IL-6

Abbreviations

ALT	Alanine aminotransferase
AST	Aspartate aminotransferase
ELISA	Enzyme-linked immunosorbent assay
ERK	Extracellular signal-related kinase
ExPH	Extended partial hepatectomy
HGF	Hepatocyte growth factor
IL-6	Interleukin-6
JNK	c-jun N-terminal kinase
LDLT	Living donor liver transplantation
PCR	Polymerase chain reaction
PH	Partial hepatectomy
STAT3	Signal transducer and activator of transcription 3
TNF	Tumor necrosis factor
VEGF	Vascular endothelial growth factor

Introduction

The liver is the human internal solid organ capable of regeneration [1, 2], enabling the performance of surgical procedures, including liver resection and living donor liver transplantation (LDLT), for primary and metastatic liver

Electronic supplementary material The online version of this article (doi:10.1007/s00535-014-0992-5) contains supplementary material, which is available to authorized users.

S. Yoshiya (✉) · K. Shirabe · D. Imai · T. Toshima · Y. Yamashita · T. Ikegami · S. Okano · T. Yoshizumi · H. Kawanaka · Y. Maehara
Department of Surgery and Science, Graduate School of Medical Sciences, Kyushu University, 3-1-1 Maidashi, Higashi-ku, Fukuoka 812-8582, Japan
e-mail: yoshiya@surg2.med.kyushu-u.ac.jp

K. Shirabe
e-mail: kshirabe@surg2.med.kyushu-u.ac.jp

Published online: 23 August 2014

tumors and end-stage liver diseases. Postoperative liver failure is a life-threatening complication after liver resection, with one risk factor for liver failure being small remnant liver volume [3, 4]. In LDLT, graft-size mismatching is a major problem, and small-for-size syndrome, characterized by prolonged hyperbilirubinemia, intractable ascites and delayed recovery of synthetic function, may lead to early graft failure [5]. Although various methods of enhancing liver regeneration have been tested [6–10], few of these have been utilized clinically.

F13A, a peptide composed of 13 amino acids, is a specific antagonist [11] and endogenous ligand of APJ, a G protein-coupled receptor [12]. The apelin–APJ system plays important roles in the regulation of cardiovascular function, inflammation, fluid homeostasis, the adipo-insular axis, and angiogenesis [13, 14]. In the liver, the apelin–APJ system was shown to be involved in hepatocyte apoptosis, collateral vessels formation in cirrhotic liver, fibrosis progression, and glycogen synthesis [15–18]. Moreover, apelin was shown to be related to the relationship between apelin and tumor necrosis factor (TNF)-α, an initiator of liver regeneration [1, 2]. These findings suggest a relationship between liver regeneration and the apelin–APJ system. To investigate this association, we assessed the impact of F13A inhibition of the apelin–APJ system on hepatocyte proliferation and liver regeneration following partial or extended partial hepatectomy in mice.

Materials and methods

Antibodies and reagents

F13A (Supplemental Fig. 1a) was purchased from Phoenix Pharmaceuticals, Inc. (Burlingame, CA, USA), and 5-bromo-2-deoxyuridine (BrdU) was obtained from Sigma-Aldrich (St. Louis, MO, USA). Primary antibodies for immunohistochemistry included rabbit anti-APJ (Santa Cruz Biotechnology, Santa Cruz, CA, USA, and Life Span Biosciences, Inc., Seattle, WA, USA), rat anti-BrdU (Abcam, Cambridge, MA, USA), rat anti-mouse CD69 (Santa Cruz Biotechnology), rat anti-mouse F4/80 (Bio-Rad AbD Serotec Ltd, Oxford, UK), and rat anti-mouse Ki-67 (DAKO, Glostrup, Denmark). All primary antibodies used in Western-blotting experiments were purchased from Cell Signaling Technology, Inc. (Danvers, MA, USA).

Animals and surgical procedures

Male C57BL/6 mice, aged 6–8 weeks (Charles River Japan) were maintained in a specific pathogen-free facility with a 12-h-dark/12-h-light cycle. All animal experiments were approved by the Kyushu University Animal Experiment Committee, and the care of the animals was in accordance with institutional guidelines.

For partial hepatectomy (PH), mice were anesthetized by inhalation of isoflurane, followed by a midline laparotomy resecting the median and left lateral lobes, removing approximately 70 % of the entire liver, as described [19]. Extended hepatectomy (ExPH) was performed similarly, except that the right middle and lower lobes were also resected, removing about 90 % of the entire liver [8]. Liver specimens and blood samples were harvested before and 1, 3, 6, 12, 24, 48, 96, and 168 h after surgery. Liver weights and body weights were also measured at these times, and liver/body weight ratios were calculated.

The effect of F13A on the PH model was tested by intraperitoneally injecting 150 μg/kg/day F13A, starting 24 h before surgery and daily until the animals were killed. The effect of F13A on the ExPH model was tested by injections 24 h before and just after surgery. To assess BrdU incorporation, mice were intraperitoneally injection with 50 mg/kg BrdU 2 h before killing.

Immunostaining

Liver samples were fixed overnight in 10 % formaldehyde, embedded in paraffin, and sectioned at a thickness of 3–4 μm. Endogenous peroxidase activity was blocked by incubating the sections in 3 % H_2O_2 in methanol, and nonspecific binding was blocked by incubation with 10 % normal goat serum (Nichirei Bioscience Inc., Tokyo, Japan). The sections were incubated overnight at 4 °C with primary antibody, washed, and incubated with the appropriate secondary antibody for 60 min at room temperature. Antigen–antibody complexes were visualized using DAB kits (DAKO). For immunocytochemistry, Kupffer cells were plated onto Lab-Tek chamber slides, fixed, and stained. As negative controls for all experiments, primary antibody was omitted. Immunostained slides were viewed under a BIOREVO BZ-9000 microscope (Keyence, Osaka, Japan). For Ki-67, BrdU, and CD69 analyses, a minimum of ten different images were randomly selected and positive cells were counted with ImageJ software (National Institutes of Health, Bethesda, MD, USA).

Assessment of activated Kupffer cells/macrophages in regenerating livers

The number of activated Kupffer cells/macrophages was assessed immunohistochemically using antibody to CD69, the earliest antigen to appear after activation of macrophages [20]. Activated Kupffer cells/macrophages were defined as CD69-positive cells of stellate or spindle shape located in the sinusoids [21].

Biochemical tests of liver function

Serum samples were obtained from the inferior vena cava just before liver harvesting after precipitation of blood cells. All measurements were performed by SRL Inc. (Tokyo, Japan).

Enzyme-linked immunosorbent assays (ELISA)

The concentrations of TNF-α and IL-6 in serum and the supernatants of cultured cells were directly determined using the Mouse TNF-alpha and Mouse IL-6 Quantikine ELISA kits, respectively (R&D Systems, Inc., Minneapolis, MN), according to the manufacturer's protocols. The concentrations of HGF in liver lysates were determined by adjusting for equal protein concentrations, followed by assays using Mouse/Rat HGF Quantikine ELISA kits (R&D Systems, Inc.), according to the manufacturer's instructions.

Quantitative real-time polymerase chain reaction

Total RNA was extracted from frozen liver tissue using RNeasy Mini kit (QIAGEN, Hilden, Germany) and reverse transcribed using SuperScriptIII (Invitrogen, Carlsbad, CA) following the manufacturers' instructions. Quantitative RT-PCR was performed using TaqMan enzyme and an Applied Biosystems 7500 real-time PCR system (Applied Biosystems, Foster City, CA, USA). The probes used are summarized in Supplemental Table 1. All samples were amplified with β-actin primers as an endogenous loading control. Results are presented as fold induction over controls.

Western blotting

Livers were lysed in RIPA buffer (Thermo Scientific, Waltham, MA, USA). Proteins (20 μg) were separated by SDS polyacrylamide gel electrophoresis and transferred to polyvinylidene difluoride membranes. The membranes were washed, blocked, and incubated with the primary antibody and then with an appropriate horseradish peroxidase-conjugated secondary antibody. The signals were visualized by enhanced chemiluminescence (Chemi-Lumi One Ultra; Nacarai Tespue, Kyoto, Japan). The images were scanned and the relative density of immunoreactive bands was determined using ImageJ software.

Isolation of primary hepatocytes and Kupffer cells and in vitro assays

Primary hepatocytes and Kupffer cells from C57BL/6 mice aged 6–8 weeks were isolated using a collagenase perfusion protocol [22]. The isolated hepatocytes were maintained on type I collagen-coated dishes at 37 °C under 5 % CO_2 in HMM medium (Lonza, Basal, Switzerland). Twenty-four hours after plating, the primary hepatocytes were treated with F13A (1 mM) for an additional 24 h. BrdU incorporation was measured with Cell Proliferation ELISA, BrdU (colorimetric; Roche Diagnostics GmbH, Mannheim, Germany), according to the manufacturer's protocol. To isolate Kupffer cells, non-parenchymal cells were labeled with anti-biotin conjugated rat anti-mouse F4/80 and passed through a magnetic separation column (Miltenyi Biotech, Auburn, CA, USA) according to the manufacturer's protocol. F4/80-positive cells were further purified by selective adherence to plastic. The resulting Kupffer cells were plated onto 24-well plates at a density of 1×10^5 cells/well in Roswell Park Memorial Institute (RPMI) 1640 medium with 10 % fetal bovine serum and treated with various concentrations of F13A for 24 h at 37 °C. Human LX-2 hepatic stellate cells (Millipore) were plated onto 24-well plates at a density of 2×10^4 cells/well and treated with F13A for 24 h at 37 °C. The supernatants were collected and stored at −80 °C.

Statistical analysis

All statistical analyses were performed using SAS software (JMP 9.0.1; SAS Institute Inc., Cary, NC, USA). All variables are expressed as mean ± standard deviation (SD), with between-group differences assessed by Student's t tests and Mann–Whitney U tests. Survival rates in the ExPH model were calculated by the Kaplan–Meier method and compared with the log-rank test. A p value of <0.05 was considered statistically significant.

Results

F13A accelerates liver regeneration after PH

The effects of F13A on liver regeneration after PH were assessed by measuring the liver weight-to-body weight ratio. Regeneration was significantly more rapid in F13A-treated than in control mice, with significantly higher ratios beginning after 24 h ($p < 0.01$) and continuing to 96 and 168 h ($p < 0.05$ each; Fig. 1a). Serum alanine aminotransferase (ALT) and aspartate aminotransferase (AST) concentrations, both markers of hepatocyte damage, peaked in both groups of mice 12 h after PH, but were significantly lower in F13A-treated than in control mice ($p < 0.05$ each; Fig. 1b). Moreover, to assess the impact of F13A on hepatocyte proliferation, hepatocyte DNA synthesis was analyzed by immunohistochemical staining of regenerating livers with well-known markers of DNA

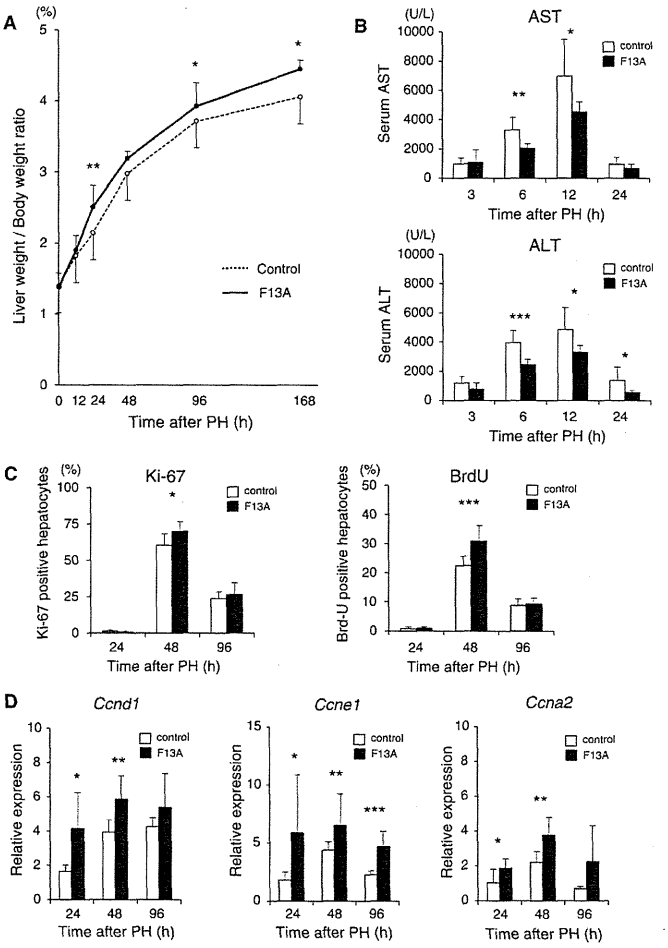

Fig. 1 F13A accelerates liver regeneration after PH. Mice were subjected to PH and treated with F13A of left untreated as described. **a** Liver weight/body weight ratio. **b** Serum AST and ALT concentrations. **c** Percentages of Ki-67- and BrdU-positive hepatocytes. **d** Real-time PCR analyses of *cyclin A2* (*Ccna2*), *cyclin D1* (*Ccnd1*), and *cyclin E1* (*Ccne1*) mRNA expression; the level in preoperative control mice was set at 1. All results are expressed as mean ± SD ($n = 6$). $^{*}p < 0.05$, $^{**}p < 0.01$, $^{***}p < 0.001$ compared with controls

replication, Ki-67 and BrdU. Although DNA synthesis in proliferating hepatocytes of both groups peaked 48 h after PH, the percentages of both Ki-67- and BrdU-positive hepatocytes were significantly higher in the F13A-treated than in control livers ($p < 0.05$; Fig. 1c).

Because cyclins are required for hepatocyte proliferation in regenerating liver, we assessed the hepatic gene expression of several cyclins. The expression of cyclins D1 (*Ccnd1*) and E1 (*Ccne1*), which peak during G_1 phase, and of cyclin A2 (*Ccna2*), which peaks during S phase, was significantly higher in F13A-treated than in control mice 24 ($p < 0.05$ each) and 48 ($p < 0.01$ each) hours after PH (Fig. 1d). These findings indicated that F13A accelerates DNA synthesis in hepatocytes, resulting in significantly enhanced hepatocyte proliferation and liver regeneration after PH.

F13A alters cytokine, but not growth factor, expression after PH

Many cytokines and growth factors play important roles in liver regeneration after PH, the most notable being IL-6

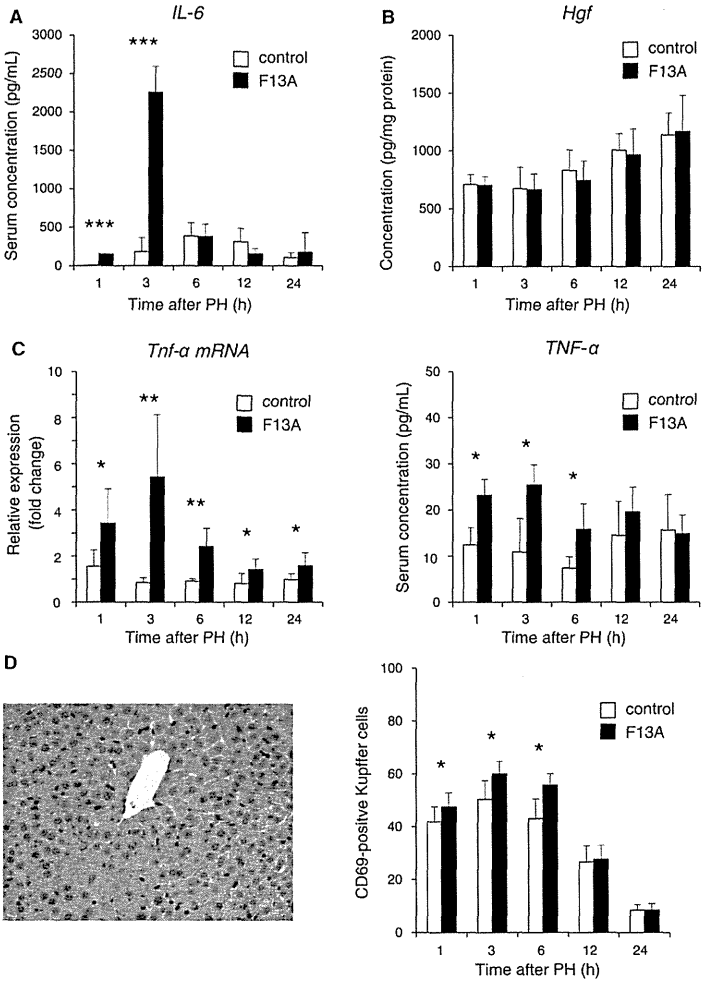

Fig. 2 Effect of F13A on the expression of IL-6, TNF-α, and HGF and on the expression of the Kupffer cell/macrophage activation marker CD69 after PH. **a, b** Serum concentrations of IL-6 and hepatic concentrations of HGF over time. **c** Hepatic TNF-α mRNA expression and serum TNF-α concentrations over time. **d** Immunohistochemical staining of regenerating liver with antibody to CD69 (*left*, original magnification ×200), and histograms representing the number of CD69-positive Kupffer cells/macrophages (*right*). All results are expressed as mean ± SD ($n = 6$). $^{*}p < 0.05$, $^{**}p < 0.01$, $^{***}p < 0.001$ compared with controls

and hepatocyte growth factor (HGF) [1, 2]. Using ELISA, we found that the serum concentration of IL-6 was significantly higher in F13A-treated than in control mice at 1 (19.6-fold, $p < 0.001$) and 3 (12.3-fold, $p < 0.001$) hours after PH (Fig. 2a), whereas there were no differences in the level of expression of hepatic HGF (Fig. 2b) or of hepatic vascular endothelial growth factor (VEGF; Supplemental Fig. 2), which is also involved in liver regeneration after PH [23].

Kupffer cells are promoted during F13A-activated liver regeneration

Because IL-6 is generated by and released primarily from Kupffer cells [1, 2], we evaluated the expression of TNF-α, a marker of activated Kupffer cells and an initiator of liver regeneration. Both hepatic gene expression and serum concentration of TNF-α after PH were significantly higher in F13A-treated than in control mice (Fig. 2c).

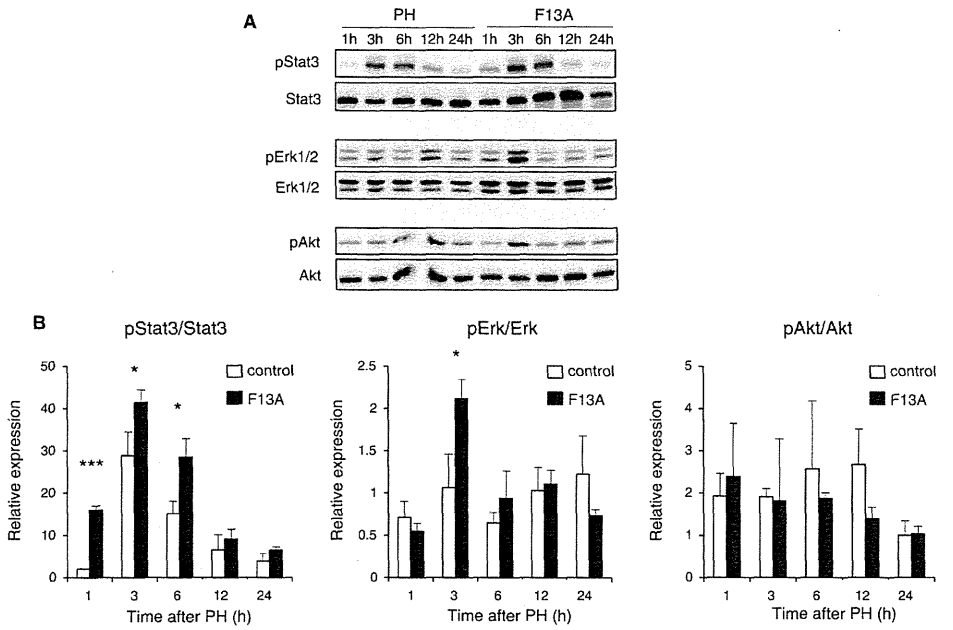

Fig. 3 F13A enhances STAT3 and Erk1/2, but not PI3 K/Akt, signaling after PH. **a** Western-blotting analysis of the phosphorylation status of STAT3, Erk1/2, and PI3 K/Akt. **b** Densitometric analysis of the results in **a**. Results were expressed as mean ± SD (n = 3), with findings in preoperative control mice set at 1. $*p < 0.05$. $***p < 0.001$ compared with controls

Furthermore, immunohistochemical staining of CD69 revealed that the number of positive Kupffer cells/macrophages in regenerating liver was significantly higher in F13A-treated than in control mice at 1, 3, and 6 h after PH ($p < 0.05$ each; Fig. 2d). These results suggest that F13A activated Kupffer cells in regenerating liver, leading to increased IL-6 secretion after PH.

F13A accelerates STAT3 and Erk1/2, but not PI3K/Akt, signaling after PH

Because intracellular signaling pathways, including the signal transducer and activator of transcription 3 (STAT3), extracellular signal-related kinase 1 and 2 (Erk1/2), and phosphatidylinositide 3 kinase (PI3 K)/Akt pathways, play important roles in cell proliferation and/or survival after PH [1, 2], we investigated the effect of F13A on these three pathways. Liver samples from F13A-treated mice showed significantly more intense phosphorylation of STAT3 [7.8-fold at 1 h ($p < 0.001$), 1.4-fold at 3 h ($p < 0.05$), and 1.9-fold at 6 h ($p < 0.05$)] and Erk1/2 [2.0-fold at 3 h ($p < 0.05$)] than samples from control mice (Fig. 3). In contrast, levels of phosphorylated Akt were similar in the two groups (Fig. 3; $n = 3$).

F13A does not induce apoptosis in regenerating liver

Because F13A increased the expression of TNF-α, an inducer of apoptosis, and because TNF-α induced apoptosis is mediated by the caspase family, we examined whether F13A could induce hepatocyte apoptosis in regenerating livers by assaying the expression of mRNAs encoding caspases-3, -8, and -9. We found that the levels of these three caspases were similar in F13A-treated and control mice (Supplemental Fig. 3; $n = 6$), as were the number of TUNEL-positive cells.

F13A does not induce inflammation in regenerating liver

Because both TNF-α and IL-6 also trigger acute inflammatory responses in hepatocytes, causing liver damage, we measured the levels of mRNA encoding the acute phase response proteins serum amyloid A1 (*Saa1*) and fibrinogen

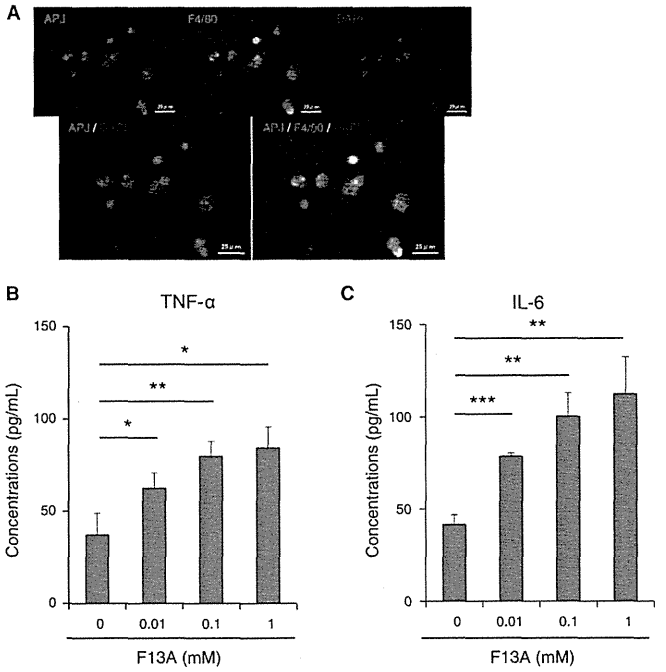

Fig. 4 F13A affects Kupffer cells directly in vitro. **a** Immunocytochemical co-staining of APJ (*red*), F4/80 (Kupffer cell marker, *green*), and DAPI (nuclei, *blue*), showing colocalization of APJ and F4/80 as *yellow*. *Scale bar* 50 μm. **b**, **c** Supernatant concentrations of TNF-α (**b**) and IL-6 (**c**) in cultured Kupffer cells treated with the indicated concentrations of F13A and analyzed by ELISA. Results are expressed as mean ± SD ($n = 3$). *$p < 0.05$, **$p < 0.01$ compared with controls

(*Fgg*) 24 h after PH [24]. The levels of both were similar in F13A-treated and control mice (Supplemental Fig. 4: $n = 6$).

F13A directly promotes the activation of Kupffer cells in vitro

Our in vivo results, demonstrating that the F13A-associated increased proliferation of hepatocytes was accompanied by the activation of Kupffer cells suggested that F13A may directly promote the activation of Kupffer cells, not hepatocytes. We therefore harvested Kupffer cells and incubated them with F13A. Isolated F4/80-positive Kupffer cells colocalized with APJ (Fig. 4a). Moreover, treatment of Kupffer cells with F13A dose-dependently and significantly increased the concentrations of TNF-α and IL-6 in the supernatant, compared with untreated cells (Fig. 4b, c).

F13A had no effects on hepatocyte proliferation and hepatic stellate cells in vitro

To evaluate the effect of F13A on hepatocyte and hepatic stellate cell proliferation, primary hepatocytes and LX-2 cells, a human hepatic stellate cell line, were incubated with F13A. BrdU incorporation experiments showed that F13A did not directly affect hepatocyte proliferation (Supplemental Fig. 5). Additionally, these cells did not secrete TNF-α or IL-6 (data not shown). In addition, F13A treatment had no effect on HGF expression by LX-2 cells (Supplemental Fig. 6).

F13A improves survival rate after ExPH

Finally, we evaluated the therapeutic significance of F13A in the regeneration of resected liver using an ExPH (over 90 %) model, in which only 10 % of hepatectomized mice were found to survive for 7 days after surgery [8]. Although only three of 20 (15 %) control mice were alive 7 days after ExPH, 10 of 20 (50 %) F13A-treated mice survived for 7 days ($p < 0.05$, Fig. 5).

Discussion

We have shown here that mouse Kupffer cells express APJ in vitro and that F13A directly promoted the activation of

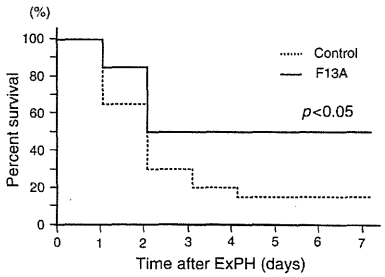

Fig. 5 F13A improves mouse survival rate following ExPH. The survival rates of F13A-treated mice and control mice were calculated by the Kaplan–Meier method and evaluated with the log-rank test

Kupffer cells, but had no direct effect on hepatocytes or hepatic stellate cells. Promotion of Kupffer cells activation enhanced the secretion of TNF-α and IL-6, resulting in increased hepatocyte proliferation and liver regeneration in the partial hepatectomy model. Finally, F13A improved the mouse survival rate in the extended partial hepatectomy model.

In liver physiology and pathology, the apelin–APJ signaling pathway has been reported to play important roles in Fas-induced liver injury, fibrosis progression, and neoangiogenesis in cirrhotic liver [15, 16]. However, the function of this signaling pathway and the impact of F13A on liver regeneration remain unclear. We found that APJ was expressed by hepatocytes and Kupffer cells, the liver's residential macrophages, in normal mouse livers, in agreement with previous results showing APJ expression in hepatocytes [15] and macrophages [25]. Interestingly, our in vitro results showed that F13A, an inhibitor of the apelin–APJ system, promoted the activation of Kupffer cells and the secretion of TNF-α. Previous studies have shown an association between the apelin–APJ system and macrophages. For example, stimulation of the apelin–APJ system in vitro reduced TNF-α secretion by macrophages [25]. NF-κB was shown to be indispensable for TNF-α release by macrophages [26], and deficiencies in the apelin–APJ system found to increase NF-κB binding [27]. These findings suggested that F13A treatment may have affected Kupffer cells by promoting the activation of NF-κB and the secretion of TNF-α.

Kupffer cells are involved in liver regeneration after PH [28–30]. Liver regeneration after PH was composed of various mechanisms and Kupffer cells were activated with PH stimulus, resulting in playing one of the roles of liver regeneration. Kupffer cells produce important growth-regulating mediators, influencing hepatocyte proliferation by paracrine mechanisms. Kupffer cell depletion was found to impair liver regeneration after PH, by decreasing TNF-α and IL-6 [28–30]. Additionally, deficiencies in type I TNF receptor and IL-6 and anti-TNF-α treatment were found to inhibit regeneration in hepatectomized mice [31–33]. Increasing the level of IL-6 was found to induce STAT3 phosphorylation and hepatocyte proliferation, resulting in massive liver growth and reduced oxidative stress [9, 34], excess TNF-α could induce apoptosis (death receptor signaling) by activating c-jun N-terminal kinase (JNK). A deficiency in APJ-signaling was found to prevent death receptor-induced apoptosis of hepatocytes by attenuating JNK activation [15]. Therefore F13A treatment did not induce apoptosis, regardless of the increased TNF-α secretion associated with the activation of Kupffer cells. Although the role of Kupffer cells in an animal model of small-for-size graft syndrome after liver transplantation remains unclear [35, 36], both studies indicated the importance of IL-6 in hepatocyte proliferation and anti-inflammatory activity. Interruption of TNF-α signaling or depletion of Kupffer cells was found to reduce reperfusion injury, but also blocked liver regeneration after transplantation because of inadequate IL-6 expression [36]. Our in vivo experiments showed that F13A did not affect the expression of the acute inflammatory response genes Saa1 and Fgg, indicating that the F13A-induced increase in IL-6 was due to its elevation of proliferation, not proinflammatory, signals. Therefore, F13A treatment may have a therapeutic effect in the model of small-for-size graft syndrome after liver transplantation by promoting the activation of Kupffer cells without inducing apoptosis or inflammation.

Growth factor- and cytokine-regulated pathways are activated during liver regeneration [2]. One of the most important growth factors is HGF, which is released by activated stellate cells. HGF binds to its receptor Met and activates the PI3 K-Akt signal-transduction pathway. Stellate cells have been associated with apelin–APJ signaling, with F13A treatment of a human hepatic stellate cell line preventing the induction of fibrogenesis-related genes by profibrogenic molecules, indicating that F13A suppresses stellate cell activation [37]. Our results showed that F13A treatment did not increase HGF expression or enhance the phosphorylation of Akt after PH and that F13A did not affect the expression of HGF by hepatic stellate cells in vitro, suggesting that F13A had no effect on stellate cells during liver regeneration.

The cytokines IL-6 and TNF-α activate neighboring hepatocytes via STAT3 and mitogen-activated protein kinase pathways. Our Western-blot analyses showed that F13A increased the levels of STAT3 and ERK1/2 phosphorylation, reflecting the elevated levels of IL-6 and TNF-α. By activating both pathways, F13A enhanced cell-cycle progression in hepatocytes, resulting in hepatocyte proliferation. Because increased hepatocyte proliferation results

in decreased serum transaminase levels [38], these decreases were likely indirect effects of F13A on hepatocytes, due to F13A promotion of Kupffer cell activation.

Our results also suggested the therapeutic possibilities of F13A in patients undergoing liver resection or LDLT. Delayed liver regeneration after massive hepatectomy or small-for-size graft transplantation could result in patient mortality. Therefore, indications for these operations are strictly restricted to patients with sufficient estimated remnant liver or graft volume. F13A treatment, by enhancing liver regeneration, may transcend current limitations on patients eligible for massive hepatectomy and on remnant liver graft volume after LDLT.

In summary, we showed that treatment with F13A, which blocks apelin–APJ signaling, promoted hepatocyte proliferation, increasing the secretion of TNF-α and IL-6 by promoting the activation of Kupffer cells during early phase of liver regeneration, and showed therapeutic effects in a mouse ExPH model. Our results suggest that F13A treatment may benefit patients undergoing liver resection and may extend criteria for both donors and recipients in LDLT.

Acknowledgments This work was supported in part by JSPS KAKENHI Grant Number 26861081.

Conflict of interest The authors declare that they have no conflict of interest.

References

1. Fausto N, Campbell JS, Riehle KJ. Liver regeneration. J Hepatol. 2012;57:692–4.
2. Taub R. Liver regeneration: from myth to mechanism. Nat Rev Mol Cell Biol. 2004;5:836–47.
3. Shirabe K, Shimada M, Gion T, et al. Postoperative liver failure after major hepatic resection for hepatocellular carcinoma in the modern era with special reference to remnant liver volume. J Am Coll Surg. 1999;188:304–9.
4. Mullen JT, Ribero D, Reddy SK, et al. Hepatic insufficiency and mortality in 1,059 noncirrhotic patients undergoing major hepatectomy. J Am Coll Surg. 2007;204:854–62.
5. Ikegami T, Shirabe K, Yoshizumi T, et al. Primary graft dysfunction after living donor liver transplantation is characterized by delayed functional hyperbilirubinemia. Am J Transplant. 2012;12:1886–97.
6. Ishiki Y, Ohnishi H, Muto Y, et al. Direct evidence that hepatocyte growth factor is a hepatotrophic factor for liver regeneration and has a potent antihepatitis effect in vivo. Hepatology. 1992;16:1227–35.
7. Ijichi H, Taketomi A, Yoshizumi T, et al. Hyperbaric oxygen induces vascular endothelial growth factor and reduces liver injury in regenerating rat liver after partial hepatectomy. J Hepatol. 2006;45:28–34.
8. Ninomiya M, Shirabe K, Terashi T, et al. Deceleration of regenerative response improves the outcome of rat with massive hepatectomy. Am J Transplant. 2010;10:1580–7.
9. Zimmers TA, McKillop IH, Pierce RH, et al. Massive liver growth in mice induced by systemic interleukin 6 administration. Hepatology. 2003;38:326–34.
10. Webber EM, Bruix J, Pierce RH, Fausto N. Tumor necrosis factor primes hepatocytes for DNA replication in the rat. Hepatology. 1998;28:1226–34.
11. Lee DK, Saldivia VR, Nguyen T, et al. Modification of the terminal residue of apelin-13 antagonizes its hypotensive action. Endocrinology. 2005;146:231–6.
12. Tatemoto K, Hosoya M, Habata Y, et al. Isolation and characterization of a novel endogenous peptide ligand for the human APJ receptor. Biochem Biophys Res Commun. 1998;251:471–6.
13. Kidoya H, Takakura N. Biology of the apelin–APJ axis in vascular formation. J Biochem. 2012;152:125–31.
14. Scimia MC, Hurtado C, Ray S, et al. APJ acts as a dual receptor in cardiac hypertrophy. Nature. 2012;488:394–8.
15. Yasuzaki H, Yoshida S, Hashimoto T, et al. Involvement of the apelin receptor APJ in Fas-induced liver injury. Liver Int. 2013;33:118–26.
16. Tiani C, Garcia-Pras E, Mejias M, et al. Apelin signaling modulates splanchnic angiogenesis and portosystemic collateral vessel formation in rats with portal hypertension. J Hepatol. 2009;50:296–305.
17. Reichenbach V, Ros J, Fernandez-Varo G, et al. Prevention of fibrosis progression in CCl4-treated rats: role of the hepatic endocannabinoid and apelin systems. J Pharmacol Exp Ther. 2012;340:629–37.
18. Chu J, Zhang H, Huang X, et al. Apelin ameliorates TNF-alpha-induced reduction of glycogen synthesis in the hepatocytes through G protein-coupled receptor APJ. PLoS One. 2013;8:e57231.
19. Higgins GM, Anderson RM. Experimental pathology of the liver: I. Restoration of the liver of the white rat following partial surgical removal. Arch Pathol. 1931;12:186–202.
20. Gavioli R, Risso A, Smilovich D, et al. CD69 molecule in human neutrophils: its expression and role in signal-transducing mechanisms. Cell Immunol. 1992;142:186–96.
21. Liu K, He X, Lei XZ, et al. Pathomorphological study on location and distribution of Kupffer cells in hepatocellular carcinoma. World J Gastroenterol. 2003;9:1946–9.
22. Seglen PO. Preparation of isolated rat liver cells. Methods Cell Biol. 1976;13:29–83.
23. Ding BS, Nolan DJ, Butler JM, et al. Inductive angiocrine signals from sinusoidal endothelium are required for liver regeneration. Nature. 2010;468:310–5.
24. da Silva CG, Studer P, Skroch M, et al. A20 promotes liver regeneration by decreasing SOCS3 expression to enhance IL-6/STAT3 proliferative signals. Hepatology. 2013;57:2014–25.
25. Leeper NJ, Tedesco MM, Kojima Y, et al. Apelin prevents aortic aneurysm formation by inhibiting macrophage inflammation. Am J Physiol Heart Circ Physiol. 2009;296:H1329–35.
26. Ringelhan M, Schmid RM, Geisler F. The NF-kappaB subunit RelA/p65 is dispensable for successful liver regeneration after partial hepatectomy in mice. PLoS One. 2012;7:e46469.
27. Han S, Englander EW, Gomez GA, et al. Pancreatitis activates pancreatic apelin–APJ axis in mice. Am J Physiol Gastrointest Liver Physiol. 2013;305:G139–50.
28. Meijer C, Wiezer MJ, Diehl AM, et al. Kupffer cell depletion by Cl2MDP-liposomes alters hepatic cytokine expression and delays liver regeneration after partial hepatectomy. Liver. 2000;20:66–77.
29. Takeishi T, Hirano K, Kobayashi T, et al. The role of Kupffer cells in liver regeneration. Arch Histol Cytol. 1999;62:413–22.
30. Abshagen K, Eipel C, Kalff JC, et al. Loss of NF-kappaB activation in Kupffer cell-depleted mice impairs liver regeneration after partial hepatectomy. Am J Physiol Gastrointest Liver Physiol. 2007;292:G1570–7.

31. Yamada Y, Kirillova I, Peschon JJ, Fausto N. Initiation of liver growth by tumor necrosis factor: deficient liver regeneration in mice lacking type I tumor necrosis factor receptor. Proc Natl Acad Sci USA. 1997;94:1441–6.
32. Brenndorfer ED, Weiland M, Frelin L, et al. Anti-tumor necrosis factor alpha treatment promotes apoptosis and prevents liver regeneration in a transgenic mouse model of chronic hepatitis C. Hepatology. 2010;52:1553–63.
33. Cressman DE, Greenbaum LE, DeAngelis RA, et al. Liver failure and defective hepatocyte regeneration in interleukin-6-deficient mice. Science. 1996;274:1379–83.
34. Jin X, Zhang Z, Beer-Stolz D, et al. Interleukin-6 inhibits oxidative injury and necrosis after extreme liver resection. Hepatology. 2007;46:802–12.
35. Yang K, Du C, Cheng Y, et al. Augmenter of liver regeneration promotes hepatic regeneration depending on the integrity of Kupffer cell in rat small-for-size liver transplantation. J Surg Res. 2013;183:922–8.
36. Tian Y, Jochum W, Georgiev P, et al. Kupffer cell-dependent TNF-alpha signaling mediates injury in the arterialized small-for-size liver transplantation in the mouse. Proc Natl Acad Sci USA. 2006;103:4598–603.
37. Melgar-Lesmes P, Casals G, Pauta M, et al. Apelin mediates the induction of profibrogenic genes in human hepatic stellate cells. Endocrinology. 2010;151:5306–14.
38. Lam SP, Luk JM, Man K, et al. Activation of interleukin-6-induced glycoprotein 130/signal transducer and activator of transcription 3 pathway in mesenchymal stem cells enhances hepatic differentiation, proliferation, and liver regeneration. Liver Transpl. 2010;16:1195–206.

Human Pathology (2014) 45, 1610–1617

ELSEVIER

Human PATHOLOGY

www.elsevier.com/locate/humpath

Original contribution

Different expression of glucose transporters in the progression of intrahepatic cholangiocarcinoma☆,☆☆

Yuichiro Kubo MD[a,b], Shinichi Aishima MD, PhD[a], Yuki Tanaka MD[a], Koji Shindo MD[a], Yusuke Mizuuchi MD[a], Koichiro Abe MD, PhD[b], Ken Shirabe MD, PhD[c], Yoshihiko Maehara MD, PhD[c], Hiroshi Honda MD, PhD[b], Yoshinao Oda MD, PhD[a,*]

[a]*Department of Anatomic Pathology, Graduate School of Medical Sciences, Kyushu University, Fukuoka 812-8582, Japan*
[b]*Department of Clinical Radiology, Graduate School of Medical Sciences, Kyushu University, Fukuoka 812-8582, Japan*
[c]*Department of Surgery and Science, Graduate School of Medical Sciences, Kyushu University, Fukuoka 812-8582, Japan*

Received 10 December 2013; revised 12 March 2014; accepted 21 March 2014

Keywords:
Glucose transporter;
Cholangiocarcinoma;
BilIN;
HIF-1

Summary Glucose transporter (GLUT)-1 is expressed in malignant tumors and correlated with poor outcome in several cancers. Biliary intraepithelial neoplasia (BilIN) is considered to be a precursor or a noninvasive lesion of invasive cholangiocarcinoma. We examined GLUT-1 and GLUT-2 expression in 149 intrahepatic cholangiocarcinomas and 39 BilINs immunohistochemically and evaluated their correlation with clinicopathological findings and patient outcome in intrahepatic cholangiocarcinoma. Furthermore, we examined the role of GLUT-1 on migration and invasion of cholangiocarcinoma cells using GLUT-1 siRNA. In intrahepatic cholangiocarcinoma, GLUT-1 expression was frequently observed near the necrotic areas, whereas GLUT-2 expression tended to be observed in adenocarcinoma of large bile ducts. Compared with the GLUT-1–negative group, the GLUT-1–positive group showed significantly larger tumor size ($P = .0031$), poor differentiation ($P < .0001$), frequent lymphatic invasion ($P = .0031$) and lymph node metastasis ($P < .0001$), and high HIF-1α expression ($P = .0297$). GLUT-2 expression was significantly correlated with good differentiation ($P = .0015$), perihilar location ($P < .0001$), perineural invasion ($P = .0049$), and lymph node metastasis ($P = .0248$). The patients with GLUT-1–positive tumors showed poor disease related survival ($P < .0001$). The numbers of migrating and invading cells were significantly decreased in GLUT-1 siRNA transfectants of cholangiocarcinoma cells. Although, GLUT-1 was expressed in all grades of BilINs, GLUT-2 was expressed only in high-grade BilINs. Our results suggest that GLUT-1 expression correlates aggressive behavior and poor prognosis, and that GLUT-1 might be a therapeutic target of cholangiocarcinoma. GLUT-2 expression may be associated with cholangiocarcinogenesis of large bile duct and is a helpful marker for detecting high-grade BilIN lesions in atypical bile ducts.

1. Introduction

Malignant cells require a steady source of energy to maintain growth and proliferation. Cancer cells preferentially use glycolysis for their energy supply, even in aerobic

☆ Disclosure/Conflict of Interest: The authors declare no conflict of interest.

☆☆ Funding disclosure: This study is supported by Grant-in-Aid for Scientific Research (C) (No.23590399) from the Japan Society for the Promotion of Science.

* Corresponding author.
E-mail address: oda@surgpath.med.kyushu-u.ac.jp (Y. Oda).

0046-8177/
http://dx.doi.org/10.1016/j.humpath.2014.03.008

conditions [1]. Glucose uptake is mediated by glucose transporters (GLUTs), and GLUT-1 expression is increased in various cancers [2-5]. Furthermore, a close relationship between high GLUT-1 expression and poor outcomes has been described in several cancers [2,6-9].

Tissue hypoxia contributes to the progression of many human cancers by inducing the up-regulation of genes associated with angiogenesis, cell survival, cell proliferation, apoptosis, and metabolism [10]. This activation is accomplished by hypoxia-inducible factors (HIFs), which accumulate in tissues under the hypoxic conditions often present in growing tumors. *GLUT-1* is a downstream target gene of HIF-1α [10,11].

Cholangiocarcinoma is the second most common type of primary liver cancer. In a previous study, GLUT-1 was a major glucose transporter in cholangiocarcinoma and was highly expressed in moderately to poorly differentiated types than in well differentiated types [12]. However, a detailed and large-scale analysis of the GLUT proteins in cholangiocarcinoma samples has never been reported. The first aim of this study was to assess whether GLUT-1 and GLUT-2 protein expression was associated with clinicopathologic and biological variables, and with outcomes.

Biliary intraepithelial neoplasia (BilIN) is considered a precursor or noninvasive lesion of invasive cholangiocarcinoma of the hilar or perihilar region. It is often difficult to diagnose BilIN lesions morphologically, and it is necessary to establish a sensitive diagnostic method. The second aim of this study was to investigate GLUT-1 and GLUT-2 expression in precursor lesions of cholangiocarcinoma.

GLUT-1 expression was correlated with higher malignant potential in several cancers. Then, the role of GLUT-1 expression in migration and invasion was examined by using GLUT-1 siRNA in cholangiocarcinoma cell lines.

2. Materials and methods

2.1. Tissue samples

Tumors and biliary lesions of the current study were surgically resected and diagnosed at the Department of Anatomic Pathology of Kyushu University from 1985 to 2008. Our study protocol was accepted by the institutional review board of Kyushu University (25-121) and conformed to the ethics guidelines of the 1975 Declaration of Helsinki. For strict privacy protection, identifying information for all samples was removed before analysis. One hundred forty-nine cases of available paraffin-embedded specimens of cholangiocarcinoma showed invasive carcinoma without special histologic features such as sarcomatoid, adenosquamous, or signet ring cells. The clinicopathologic features of the cholangiocarcinoma group are summarized in Table 1. We followed up the patients for more than 5 years and examined their disease-related survival.

Table 1 Clinicopathological features of cholangiocarcinoma

Age (y), range (mean)	33-90 (64)
Sex, male/female	95/54
HBsAg, +/-	16/133
HCV Ab, +/-	31/118
Cirrhosis, +/-	17/132
Hepatolithiasis, +/-	8/141
Tumor size (cm), range (mean)	1.0-16.5 (4.7)
Location, peripheral/perihilar	96/53
Mass-forming/non–mass-forming	106/43
Histology, well/moderate/poorly	42/63/44
Necrosis extent (%), range (mean)	0-80 (14.2)
Lymphatic invasion, +/-	73/76
Perineural invasion, +/-	83/66
Lymph node metastasis, +/-	40/109

We also selected 39 cases of BilIN (27 hepatolithiasis, 8 primary sclerosing cholangitis, and 4 cholangiocarcinoma). BilIN lesions were graded based on the histopathological definitions of BilIN [13] and classified as BilIN-1 (n = 20), BilIN-2 (n = 11), and BilIN-3 (n = 8).

2.2. Immunohistochemical staining and evaluation

Immunohistochemical staining was performed with the Envision Plus system and DAB kit (Dako, Glostrup, Denmark). The primary antibodies were anti–GLUT-1 (rabbit polyclonal, 1:300; ab15309, Abcam, Tokyo, Japan), anti–GLUT-2 (mouse monoclonal, 1:1000; ab85715, Abcam), and anti–HIF-1α (mouse monoclonal, 1:300; Novus Biologicals, Littleton, CO). After the inhibition of endogenous peroxidase and antigen retrieval with a microwave in citrate buffer (pH6.0) at 99°C for 15 min for GLUT-1 and GLUT-2 and for 20 min for HIF-1α, the sections were exposed to each primary antibody at 4°C overnight, followed by the secondary antibody/peroxidase-linked polymers. The sections were then reacted in 3,3′-diaminobenzidine, counterstained with hematoxylin. The immunohistochemical results were scored by 2 pathologists (Y.K. and S.A.) without knowledge of the clinical data. In the membranous staining of GLUT-1, membranous and/or cytoplasmic staining of GLUT-2, and nuclear staining of HIF-1α, the percentage of positive cells was estimated by a count of 1000 tumor cells in areas with most intense staining. The protein expression of GLUT-1 and GLUT-2 was limited in most cholangiocarcinoma; therefore, the cutoff value was defined as very low level. The median of membranous GLUT-1–positive cells in cholangiocarcinoma was 3% (range, 0%-80%). A case was placed into a positive group when >3% of cells showed GLUT-1 staining or into a negative group when ≤3% of cells were stained. In GLUT-2, we assessed it as positive when there was any staining of tumor cell membrane and/or cytoplasm. We used the red blood cells for positive control of GLUT-1 and hepatocytes for positive control of GLUT-2.

Table 2 Clinicopathologic correlation with GLUT1 and GLUT2 expression

	GLUT-1		P	GLUT-2		P
	Positive (n = 69)	Negative (n = 80)		Positive (n = 31)	Negative (n = 118)	
Age	64.4 ± 1.25 [a]	63.0 ± 1.16 [a]	.4367	64.7 ± 1.88 [a]	63.4 ± 0.95 [a]	.5341
Sex, male/female	41/28	54/26	.3065	19/12	76/42	.748
Tumor size, cm	5.44 ± 0.32 [a]	4.14 ± 0.29 [a]	.0031 *	3.83 ± 0.48 [a]	4.98 ± 0.25 [a]	.0326 *
Location, peripheral/perihilar	43/26	53/27	.6174	7/24	89/29	<.0001 *
Mass-forming/non–mass-forming	52/17	54/26	.2894	11/20	95/23	<.0001 *
Histology, well/moderate/poorly	6/30/33	36/33/11	<.0001 *	16/12/3	26/51/41	.0015 *
Necrosis extent, %	25.22 ± 2.27 [a]	4.89 ± 2.28 [a]	<.0001 *	10.32 ± 4.07 [a]	15.27 ± 2.10 [a]	.2824
Lymphatic invasion +/-	43/26	30/50	.0031 *	20/11	53/65	.0557
Perineural invasion +/-	45/24	38/42	.0293 *	24/7	59/59	.0049 *
Lymph node metastasis +/-	30/39	10/70	<.0001 *	13/18	27/91	.0248 *

[a] Mean ± SD.
* $P < .05$.

2.3. Cell culture and siRNA transfection

Human cholangiocarcinoma cell lines RBE and Huh28 were obtained from the Riken Bioresource Center, Tsukuba, Japan, and cultured in Dulbecco's modified Eagle's medium as recommended by the supplier. The media were purchased from Invitrogen (Carlsbad, CA) and contained 10% fetal bovine serum. Each cell line was maintained in a 5% CO_2 atmosphere at 37°C. GLUT-1 siRNA (5′-CTCCACGAGCATCTTC-GAG-3′) (product name: Hs_SLC2A1_6) and negative control siRNA, both purchased from Qiagen, were transfected using Lipofectamine 2000 (Invitrogen) and following the manufacturer's instructions.

2.4. RNA extraction and quantitative real-time RT-PCR

Total RNA was extracted from each cell line using the RNeasy Mini kit (Qiagen). Quantitative real-time reverse transcriptase polymerase chain reaction (RT-PCR) was performed using a QuantiTect SYBR Green RT-PCR kit (Qiagen) with an ABI 7500 real-time PCR system (Applied Biosystems) for 40 cycles for 15 seconds at 94°C and for 30 seconds at 55°C and 34 seconds at 72°C, according to the manufacturer's protocol. The level of mRNA in each sample was calculated from a standard curve constructed with total RNA from the Huh28 human cholangiocarcinoma cell line. The level of GLUT-1 mRNA was normalized to that of β-actin RNA. The specific primers for GLUT-1 and β-actin were obtained from Qiagen (QT00068957, QT01680476).

2.5. Cell migration and invasion assay

Cell migration was evaluated using a BD Falcon cell culture insert, and cell invasion was evaluated using a BD BioCoat Matrigel Invasion Chamber (Becton Dickinson, Franklin Lakes, NJ). The cells were harvested 48 hours after transfection, resuspended in Dulbecco's modified Eagle's medium and then added to the upper chamber at a density of 5×10^4 cells per well. Cell migration was determined after 18 hours of culture at 37°C, and cell invasion into the Matrigel was determined after 24 hours of culture at 37°C. The membrane containing migrating and invading cells was fixed and was quantified by light microscopy after removing the non-migrating and -invading cells. We counted 5 fields (×200) of migration and invasion cells and calculated the average number of cells in each field. The experiments were performed in triplicate.

Table 3 Survival analysis

	Univariate analysis	Multivariate analysis		
	P	Hazard ratio	95% CI	P
GLUT-1	<.0001 *	0.69	0.37-1.26	.2289
Tumor size	<.0001 *	0.49	0.26-0.92	.0945
Histological differentiation	.0001 *	0.38	0.21-0.68	.0834
Necrosis extent	<.0001 *	0.86	0.47-1.51	.3055
Lymphatic invasion	<.0001 *	0.54	0.25-1.08	.0009 *
Perineural invasion	.0055 *	0.61	0.34-1.09	.6
Lymph node metastasis	<.0001 *	0.74	0.41-1.32	.0276 *

Abbreviation: CI, confidence interval.
* $P < .05$.